LARGE-EDDY SIMULATION OF COMPRESSIBLE TURBULENT FLOW IN A CONVERGENT-DIVERGENT NOZZLE WITH ISOTHERMAL WALL

Susila Mahapatra, Tennyson J.A., Somnath Ghosh
Department of Aerospace Engineering,
Indian Institute of Technology, Kharagpur, India

ASTRACT

We present results from high-order accurate LES of compressible flow through a convergent-divergent nozzle with isothermal wall and circular cross-section. The incoming flow is a turbulent, subsonic fully-developed pipe flow at $M = 0.37$ and friction Reynolds number 214. A smooth transition from subsonic to supersonic flow occurs in the nozzle, accompanied by a general reduction of turbulence intensities. However, in the initial stages of expansion in the convergent part, we note a decrease in axial Reynolds stresses and a simultaneous increase in the azimuthal and radial Reynolds stresses.

INTRODUCTION

Compressible wall-bounded turbulent flows have important applications in high-speed flight. Development of accurate Reynolds stress models for compressible flows is still a challenging task, particularly the modelling of pressure-strain correlations. Recent DNS of supersonic channel flows with isothermal walls (Coleman *et al.*, 1995; Foysi *et al.*, 2004) have revealed that compressibility effects manifest themselves as mean density and temperature variations in the near-wall region. The reduction of pressure-strain correlations at supersonic Mach numbers leads to an increase in Reynolds stress anisotropy (Foysi *et al.*, 2004). Similar observations were also made in DNS of supersonic pipe flow with isothermal wall (Ghosh *et al.*, 2010). Effects of mean dilatation and extra rates of strain add further complications to supersonic flows and lead to changes in the turbulence structure which cannot be explained only by mean property variations. Such effects were described by Bradshaw (1974) and observed in LES and DNS of canonical supersonic nozzle and diffuser flows where fully developed supersonic pipe flow serves as inflow (Ghosh *et al.*, 2008; Ghosh & Friedrich, 2014). It was observed that the Reynolds stresses decrease dramatically in the nozzle and increase in the diffuser. The pressure-strain correlations were found to play a pivotal role in changing the Reynolds stresses in these flows. In the present study, we perform LES of flow through a convergent-divergent nozzle with a subsonic, turbulent pipe flow as inflow condition. The objective is to study the transition of the flow from the subsonic to the supersonic state in the present nozzle and to observe the changes in turbulence structure during this transition.

MATHEMATICAL AND COMPUTATIONAL DETAILS

The governing equations equations for compressible flow written in generalized curvilinear coordinates in a characteristic form (Sesterhenn, 2001) involving the primitive variables pressure, velocity and entropy are solved using the 6th order compact central finite difference scheme of Lele (1992) to discretise the spatial derivatives. Time integration is carried out using a low-storage 3rd order Runge-Kutta scheme (Williamson, 1980). An explicit filtering variant of the approximate deconvolution method is used for LES (Mathew *et al.*, 2003). This method has been validated with DNS data for compressible channel flow in Mathew *et al.* (2003), where it was shown that the LES data converged towards the DNS data with increasing resolution. This LES approach has also been used to study supersonic flow through pipe, nozzle and diffuser (Ghosh *et al.*, 2008). The flow configuration studied here consists of a convergent-divergent (C-D) nozzle where inflow conditions are from a fully-developed subsonic turbulent pipe flow having centerline Mach number of 0.37 and friction Reynolds number of 214. The incoming pipe flow result from a separate simulation using streamwise periodic boundary conditions. The pipe flow and nozzle flow simulations are run simultaneously and are coupled using MPI routines and the concept of characteristics. The pipe and nozzle (diffuser) flow domains are each of size $10R \times 2\pi R \times R$ in axial(x), circumferential (θ) and radial (r) directions and are discretized using $64 \times 64 \times 50$ points. The walls of the pipe and the nozzle are isothermal and are kept at the same temperature, $T_w = 276K$. Partially non-reflecting outflow conditions, based on characteristics following Poinsot & Lele (1992), are prescribed for the nozzle. The area distribution of the nozzle is specified using isentropic streamtube equations as described in Ghosh *et al.* (2008).

RESULTS

We first present instantaneous axial and azimuthal velocity fluctuations in an axial-radial plane in the nozzle in figures 1 and 2. We notice the elongation of the near-wall streamwise structures as the flow proceeds along the nozzle and undergoes acceleration and expansion. We now look at the variation of mean flow quantities in the C-D nozzle. Figure 3 (left) shows the area distribution and also the variation of mean centerline Mach number along the nozzle. The Mach number reaches a values of nearly 1.8 at the exit of the nozzle from its values of about 0.37 at the inlet. We also

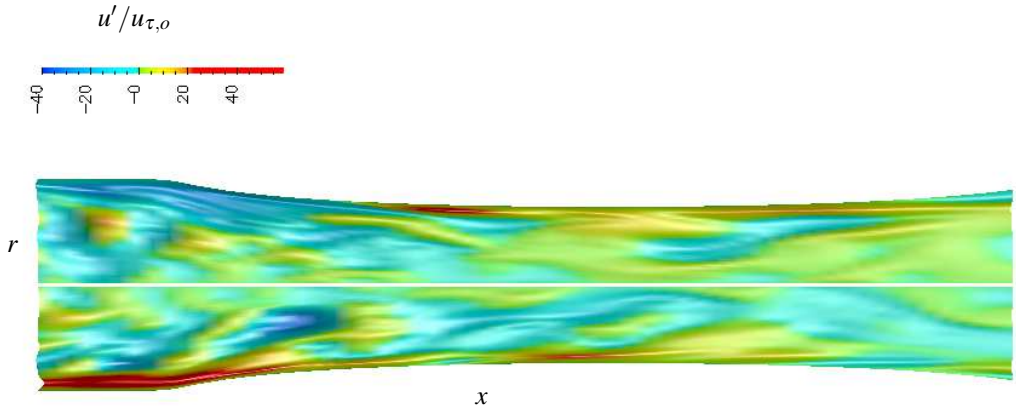

Figure 1. Axial Velocity fluctuations in an axial-radial ($x-r$) plane in the C-D nozzle, normalized with the friction velocity at inlet.

observe a monotonic (and nearly linear) increase in Mach number in the throat region. The centerline and wall mean pressure profiles (fig. 3, right) lie close to each other which indicates a nearly uniform pressure distribution along the radius. The mean density profiles at the wall and the centerline (fig. 4, left) diverge from each other as the flow becomes supersonic. The isothermal wall boundary condition implies a strong mean temperature gradient (and hence a mean density gradient) in the wall-normal direction close to the wall which is demonstrated in fig. 4, right. We note that due to the expansion in the nozzle and also due to the fact that the wall temperature along the nozzle is constant, we have a lower temperature in the core region of the nozzle compared to that at the wall. The corresponding mean density profiles in the radial direction are shown in figure 5, right. Here we also notice that the mean density distribution in the radial direction in this flow is approximately inversely proportional to the mean temperature, since the mean pressure in the radial direction remains essentially constant. The mean local Mach number profiles (fig. 5, left) demonstrate how the flow goes from subsonic to supersonic state in the nozzle. We notice how the flow close to the wall attains larger Mach numbers as we proceed along the nozzle. The axial Reynolds stress (fig.6, left) shows a large decrease along the nozzle from its value at the inlet. This trend is also seen in the azimuthal and radial stress components (fig. 6, right, fig. 7, left) at various axial locations in the nozzle except at $x/L = 0.25$ where the flow acceleration begins. At this location, we observe an increase in these stresses although the axial stress decreases. The Reynolds shear stress profiles are shown in fig. 7, right, where we notice a decay along the nozzle. At $x/L = 0.25$, the shear stress becomes negative close to the wall.

CONCLUSIONS

Large-eddy simulations of compressible flow through a canonical convergent-divergent nozzle with isothermal wall and circular cross-section at friction Reynolds number 214 (at inflow) has been performed using 6th-order accurate compact central schemes. Approximate deconvolution method based on explicit filtering has been used as the LES approach. Fully-developed low-subsonic turbulent pipe flow has been used at the inflow and the evolution of mean quantities and turbulence intensities are presented. The mean flow demonstrates the effects of expansion i.e. decrease in density, pressure, temperature along the nozzle. Turbulence intensities show a general decay along the nozzle which is expected, although in the convergent portion we find that although the axial Reynolds stresses decay, the radial and azimuthal components show an increase. This counter-intuitive behaviour needs to be explained and this is the goal of future work.

REFERENCES

Bradshaw, P. 1974 The effect of mean compression or dilatation on the turbulence structure of supersonic boundary layers. *Journal of Fluid Mechanics* **63**, 449–464.

Coleman, G. N., Kim, J. & Moser, R. D. 1995 A numerical study of turbulent supersonic isothermal-wall channel flow. *Journal of Fluid Mechanics* **305**, 159–183.

Foysi, H., Sarkar, S. & Friedrich, R. 2004 Compressibility effects and turbulence scalings in supersonic channel flow. *Journal of Fluid Mechanics* **509**, 207–216.

Ghosh, S., Foysi, H. & Friedrich, R. 2010 Compressible turbulent channel and pipe flow: similarities and differences. *Journal of Fluid Mechanics* **648**, 155–181.

Ghosh, Somnath & Friedrich, Rainer 2014 Effects of distributed pressure gradients on the pressure-strain correlations in a supersonic nozzle and diffuser. *Journal of Fluid Mechanics* **742**, 466–494.

Ghosh, S., Sesterhenn, J. & Friedrich, R. 2008 Large-eddy simulation of supersonic turbulent flow in axisymmetric nozzles and diffusers. *International J. of Heat and Fluid Flow* **29**, 579–590.

Lele, S.K. 1992 Compact finite difference schemes with spectral-like resolution. *Journal of Computational Physics* **103**, 16–42.

Mathew, J., Lechner, R., Foysi, H., Sesterhenn, J. & Friedrich, R. 2003 An explicit filtering method for large eddy simulation of compressible flows. *Physics of Fluids* **15**, 2279–2289.

Poinsot, T. J. & Lele, S. K. 1992 Boundary conditions for direct simulations of compressible viscous flows. *Journal of Computational Physics* **101**, 104–129.

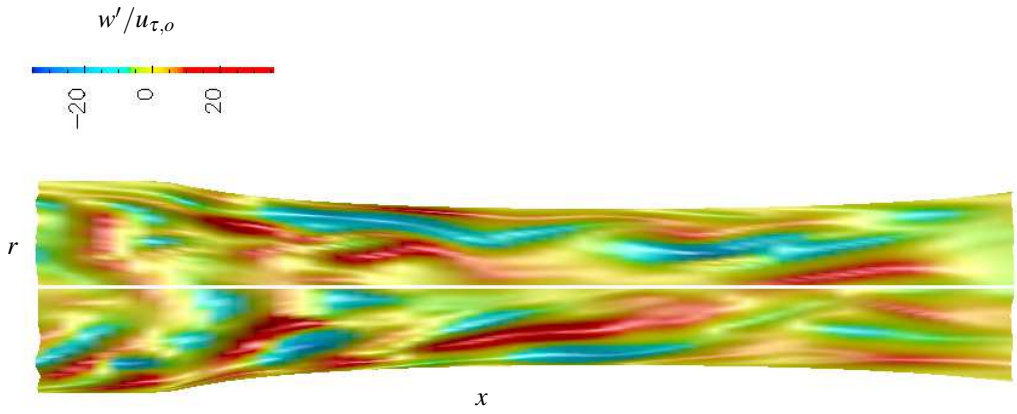

Figure 2. Azimuthal velocity fluctuations in an axial-radial ($x-r$) plane in the C-D nozzle, normalized with the friction velocity at inlet.

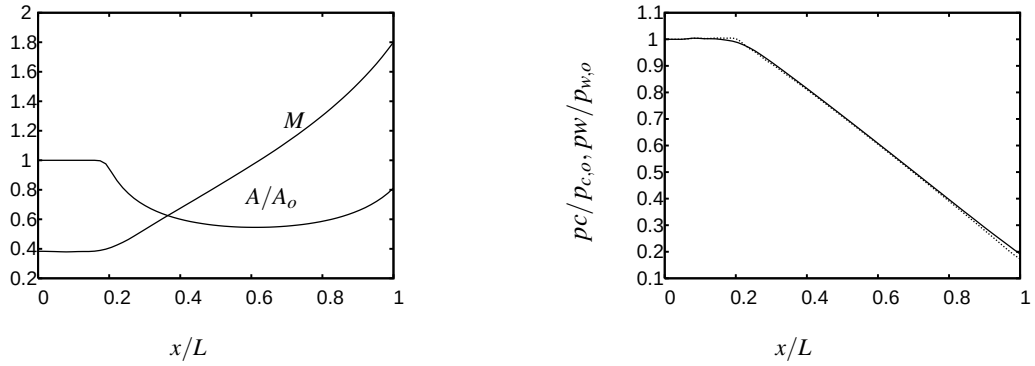

Figure 3. Area distribution, centerline Mach number (left); Mean centerline pressure (solid line), wall pressure (dashed line) in the nozzle normalized with their inlet values.

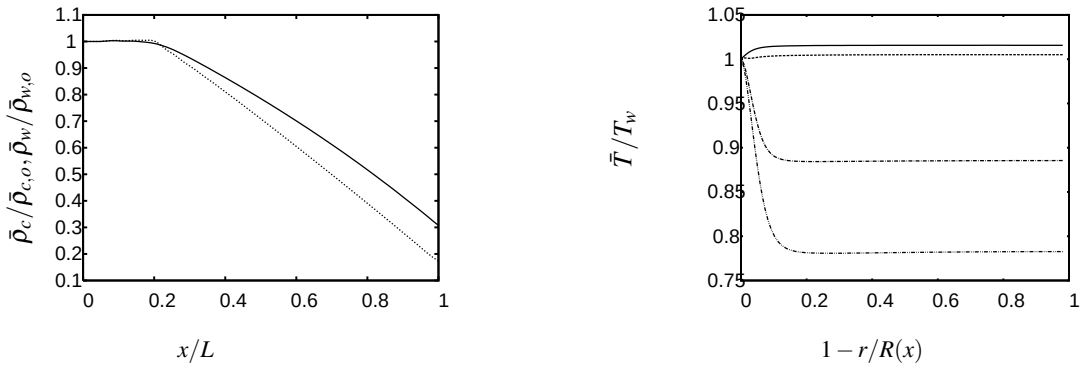

Figure 4. Mean centerline (solid line) and wall density (dashed line) normalized with their values at inlet (left); Mean temperature profiles at — $x/L=0.01$, ... $x/L=0.25$, -.-.- $x/L=0.6$ and .. .. .. $x/L=0.8$ (right), in the nozzle

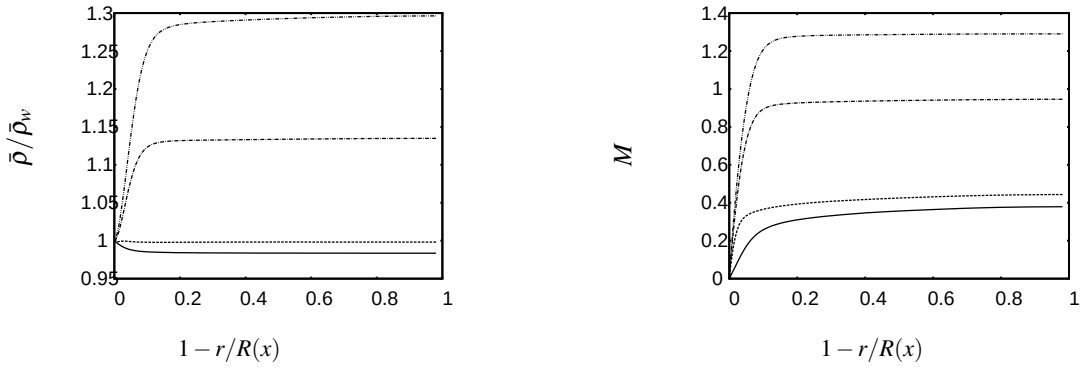

Figure 5. Mean density (left) and mean Mach number (right) profiles at — $x/L = 0.01$, ... $x/L = 0.25$, -.-.- $x/L = 0.6$ and .. .. .. $x/L = 0.8$ in the nozzle.

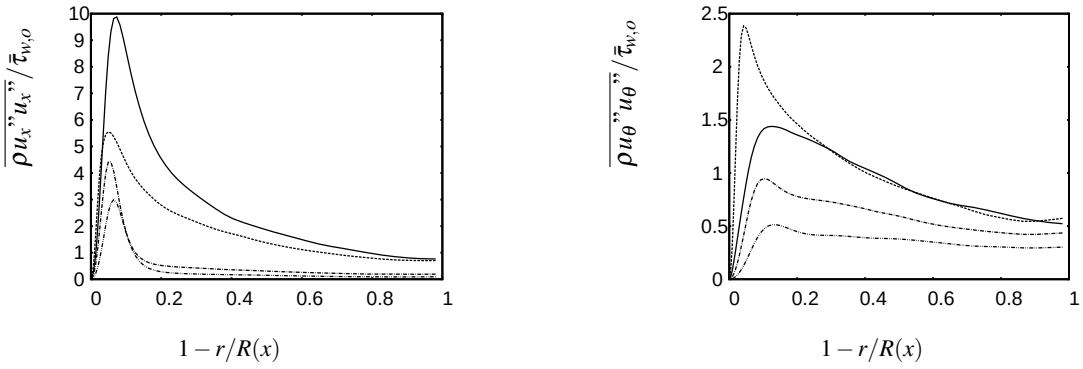

Figure 6. Axial (left) and azimuthal (right) Reynolds stress profiles at — $x/L = 0.01$, ... $x/L = 0.25$, -.-.- $x/L = 0.6$ and .. .. .. $x/L = 0.8$ in the nozzle.

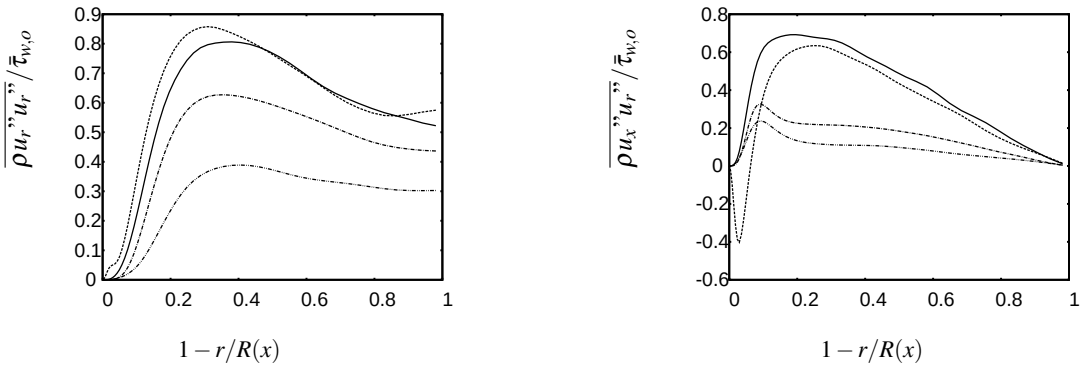

Figure 7. Radial Reynolds stress (left) and Reynolds shear stress (right) profiles in the nozzle. Line types as in figure 6

Sesterhenn, J. 2001 A characteristic-type formulation of the Navier-Stokes equations for high order upwind schemes. *Computers and Fluids* **30**, 37–67.

Williamson, J. K. 1980 Low-storage Runge-Kutta schemes. *Journal of Computational Physics* **35**, 48–56.